第 43 卷 第 7 期/2023 年 4 月/光学学报 研究论文

光学学报

基于改进GS算法设计DOE制备紫外波段微米级均匀光斑

张玉莹，赵帅*，郑昕

季华实验室，广东 佛山 528200

摘要 利用衍射光学元件(DOE)对紫外激光进行相位调制，可在远场衍射获得微米级均匀光斑。该方法的优点为：可灵活设计均匀光斑的形状、尺寸；具有较高的能量损伤阈值，适用于高功率光源。DOE设计的难点在于制备微米级均匀光斑的同时，兼顾陡度、均匀度等参数指标。基于解析法设计DOE生成的均匀光斑过渡区陡度变化缓慢，可有效利用的均匀区域较小，不适合制备小尺寸均匀光斑。此外，基础Gerchberg-Saxton(GS)算法制备微米级平顶光束，整形效果不明显，均匀度无法满足应用要求。将基础GS算法收敛结果作为改进GS算法的初始相位，改进GS算法在频域设置信号区和噪声区，并限制频域振幅分布，在理论上具备可行性。分析了离焦误差影响，并进行了实验验证，发现实验结果与理论结果具有一致性。

关键词 激光光学；DOE设计；修正GS算法；平顶光束整形；激光加工

中图分类号 O436 **文献标志码** A **DOI**：10.3788/AOS221714

1 引 言

激光器光源一般为高斯强度分布，其能量集中的特点在激光钻孔[1]、MicroLED修复与转移[2]和激光切割[3]等微精密加工领域中会导致样品表面能量密度不均匀、材料损坏等问题出现[4]。光束整形的研究大致分为两类，一类是折射方法，另一类是衍射方法。折射元件是指透镜组合，包括球面和非球面，基于几何光学理论，无需配合聚焦透镜使用[5-6]，通常应用于晶片检查或传感等领域，其特点为：输出均匀光斑尺寸近似入射光束直径(光强下降为$1/e^2$)；只能在短距离传输内保持平顶分布，自由空间远距离传输则变为贝塞尔光束[7]。

衍射方法基于衍射光学元件(DOE)调节光束波前相位，将衍射光学元件放置在聚焦透镜之前，则在透镜后焦面上可获得均匀的光强分布[8-9]，该方法可灵活设计均匀光斑的形状、尺寸，具有较高的自由度。因此，本文基于DOE制备微米级均匀光斑，根据衍射极限原理，选择紫外波段作为光源。制备小尺寸均匀光斑的DOE设计难点在于得到满足陡峭锐利的过渡区和平顶区域均匀度小于5%的特性参数。基于解析方法设计DOE，均匀光斑过渡区变化缓慢，可有效利用的均匀区域的宽度与直径相差较大，不适合制备小尺寸均匀光斑，故采用数值分析方法设计DOE。数值分析方法中有效的是迭代傅里叶算法，包括Gerchberg-Saxton(GS)算法及其各种改进算法[10-12]。基础GS算法原理逻辑清晰，空域、频域和评价函数的限制条件均可调整，设计自由度较高，是DOE设计中的有效工具。

利用基础GS算法设计DOE来制备均匀光斑，由于目标均匀光斑尺寸接近衍射极限，故整形效果不明显，均匀度无法满足参数要求。因此，本文采用基础GS算法与改进GS算法相结合的方式。首先，采用基础GS算法计算DOE初级相位分布，将此相位作为改进GS算法的初始相位。然后，利用改进GS算法在频域设置信号区和噪声区，并限制频域振幅变化，收敛结果即为DOE最终相位分布。最后，委派合作单位基于全息图加工制作DOE，并设计实验对DOE元件进行实验验证。

2 基本原理

将均匀光斑归一化光强I在0.95～1.00范围内的区域定义为平顶区域，将归一化光强I在0～0.95范围的区域定义为过渡区，将过渡区光强曲线的斜率定义为陡度。设入射高斯光束为$E_{in}(x,y)=\exp\left[-\left(x^2+y^2\right)/w_0^2\right]$，其中$w_0$为束腰半径。聚焦透镜后焦面对应频域坐标$(u,v)$，基于DOE制备均匀光斑

收稿日期：2022-09-16；**修回日期**：2022-10-21；**录用日期**：2022-11-25；**网络首发日期**：2023-01-04

基金项目：国家重点研发计划(2021YFB3602600)

通信作者：*zs040148@163.com

$E_{uni}(x_2,y_2)$的原理为

$$E_{uni}(x_2,y_2)=\mathcal{F}\left\{E_{in}\exp\left[i\varphi(x,y)\right]\right\},\tag{1}$$

式中：$\varphi(x,y)$为DOE相位分布；$\mathcal{F}(\cdot)$为快速傅里叶变换(FFT)函数。

利用超高斯函数定义目标方形均匀光斑，记为

$$E_{uni}(x_2,y_2)=\mathrm{rect}(x_2,y_2,2w_f)\exp\left(-\frac{x_2^2+y_2^2}{w_f^2}\right)^n,\tag{2}$$

式中：w_f为均匀光斑束腰半径；n为阶数；rect(·)为矩形窗函数。仿真系统参数设定为：入射光束光源波长为λ=355 nm、束腰半径为w_0=1.5 mm，均匀光斑束腰半径为w_f=12 μm，阶数为n=24。此外，聚焦透镜焦距为F=100 mm。

光束整形效果的评价参数有均匀度(Uni)和均方根误差(RMSE)，定义为

$$\begin{cases}U_{ni}=\dfrac{I_{max}-I_{min}}{I_{max}+I_{min}}\times 100\%\\ E_{RMS}=\sqrt{\dfrac{\sum_{i=1}^{N}\sum_{j=1}^{M}(I_{ij}-\bar{I})^2}{MN}}\end{cases},\tag{3}$$

式中：I_{max}为最大光强；I_{min}为最小光强；M和N为光强数据矩阵行列数；I_{ij}为任一位置光强数据；$\bar{I}$为所有光强数据的均值。

根据Uni和RMSE，对比分析解析法、基础GS算法和改进GS算法的DOE整形效果。

2.1　解析法

将入射高斯函数先整形为sinc函数，经过FFT后衍射光斑为圆形平面光场。DOE的透过率为

$$T_1=\begin{cases}\exp(iq_1\pi), & -q_2w_0\leqslant w\leqslant q_2w_0\\ 0, & \text{else}\end{cases},\tag{4}$$

式中：q_1和q_2为常数，一定范围内高斯光束中心区域与边缘区域复振幅的符号相反[13]。在仿真中设定q_1=1.00、q_2=1.27、DOE视场范围为$L=12\times 2w_0$和采样点为N=7680，光束整形结果如图1所示。此时，生成的均匀光斑直径为21.8 μm，过渡区曲线陡度为89.36°，平顶宽度为10.08 μm(直径的46.24%)，U_{ni}=0.0945，E_{RMS}=0.1061。虽然可以通过改进DOE透过率函数将圆形均匀光斑改为方形，但是均匀光斑的尺寸是根据入射光斑尺寸和光学系统参数确定的，约束性较强。

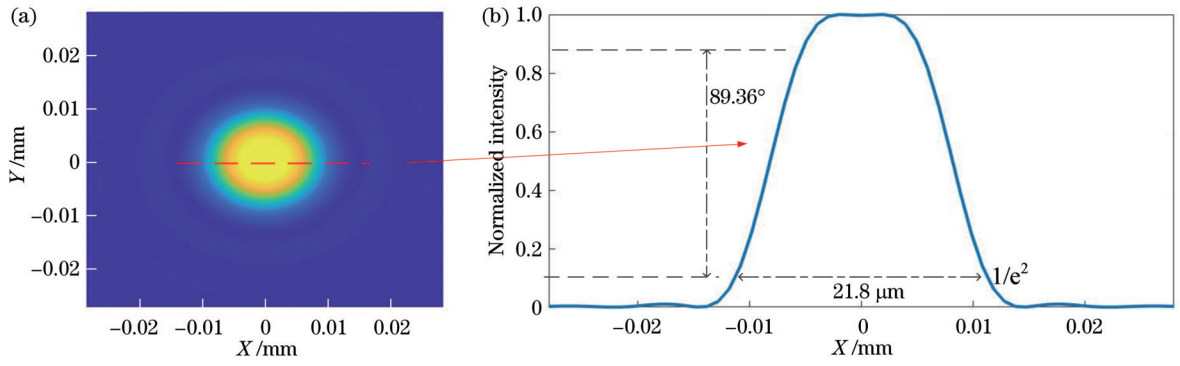

图1　解析法设计DOE的光束整形效果。(a) XY平面光强二维分布图；(b) Y=0中心线光强包络曲线

Fig. 1　Beam shaping effect of analytical designed DOE. (a) Two-dimensional distribution of light intensity in XY plane; (b) light intensity envelope curve of Y=0 center line

2.2　基础GS算法

利用基础GS算法设计DOE相位，初始相位会影响GS算法的迭代次数和收敛速度，容易陷入局部最优解。基于空间滤波原理计算初始相位可降低迭代次数[14-15]，详细介绍如下。

在2-f系统中，光场某一鞍点附近邻域内，振幅分布$a(x,y)$变化缓慢，带有相位$\varphi_a(x,y)$，傍轴近似条件下局部空间频率(u_a,v_a)可表示为

$$\begin{cases}u_a=\dfrac{1}{2\pi}\cdot\dfrac{\partial\varphi_a(x,y)}{\partial x}\\ v_a=\dfrac{1}{2\pi}\cdot\dfrac{\partial\varphi_a(x,y)}{\partial y}\end{cases},\tag{5}$$

坐标(x_2,y_2)表示透镜后焦面，由夫琅禾费衍射$(x_2=u_aF\lambda, y_2=v_aF\lambda)$可得

$$\begin{cases}\dfrac{F}{k}\cdot\dfrac{\partial\varphi_a(x,y)}{\partial x}=x_2\\ \dfrac{F}{k}\cdot\dfrac{\partial\varphi_a(x,y)}{\partial y}=y_2\end{cases},\tag{6}$$

式中：$k=2\pi/\lambda$为波数。对式(6)积分即可得到相位$\varphi_a(x,y)$的表达式。参考上述过程，设定基础GS算法得到的DOE初始相位[15](便于循环快速收敛的数学计算，无物理层面含义)为

$$\varphi_0=\frac{k}{F}\left(x_2x+y_2y\right)。\tag{7}$$

仿真建模上述系统参数，在FFT计算过程中，为了在提高精度的同时贴合实际情况，设定DOE有效孔径范围为$L=5\times 2w_0$和采样点数为N=1024。基础GS算法的循环次数为30，算法收敛至稳定后得到的

衍射光斑分布如图 2 所示。

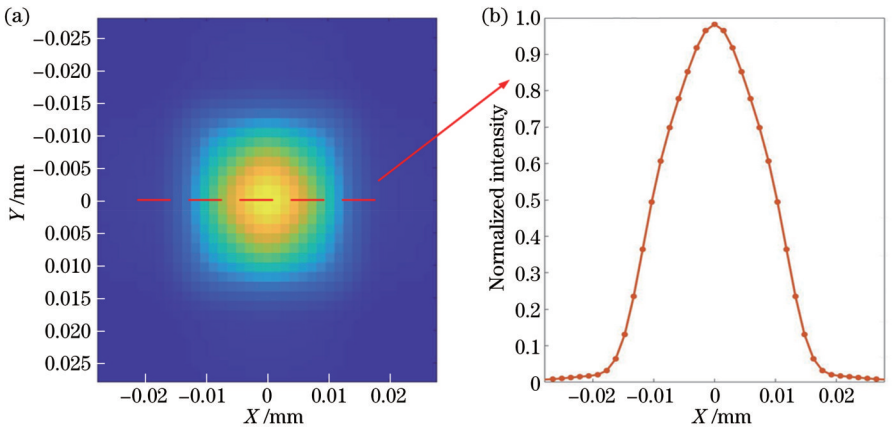

图 2　基础 GS 算法光束整形效果。(a) XY 平面光强二维分布图；(b) $Y=0$ 中心线光强包络曲线

Fig. 2　Beam shaping effect of basic GS algorithm. (a) Two-dimensional distribution of light intensity in XY plane; (b) light intensity envelope curve of $Y=0$ center line

仿真结果表明，利用基础 GS 算法设计 DOE 得到的均匀光斑存在整形效果不理想和未改变高斯强度分布的缺陷，故无法满足参数要求。参考 Wyrowski 的理论[16]，即仅通过闪耀光栅相位无法将高斯光束整形为均匀光斑，故基础 GS 算法得到正确相位的前提是这个闪耀光栅相位理论上是存在的。因此，除了相位自由度外，增加振幅自由度来改进 GS 算法也可以提高光束整形效果。

2.3　改进 GS 算法

设光场 $g(x_2,y_2)$ 包含了目标均匀光斑 $E_{\text{uni}}(x_2,y_2)$，将均匀光斑所在范围定义为窗口区 S，其余范围定于为噪声区[17]，二者之间的关系示意图如图 3 所示。

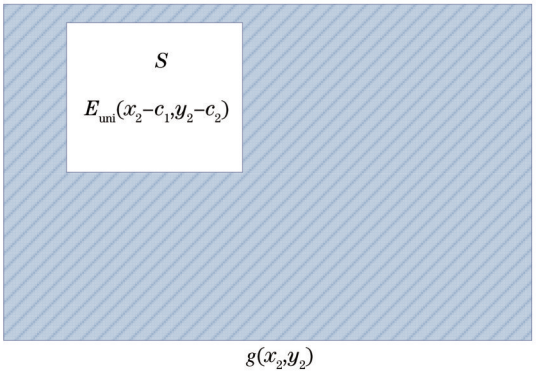

图 3　信号区与噪声区关系图示

Fig. 3　Diagram of relationship between signal area and noise area

噪声区内没有信号，故

$$g(x_2,y_2)=E_{\text{uni}}(x_2-c_1,y_2-c_2)+c(x_2,y_2), \tag{8}$$

$$\begin{cases} c(x_2,y_2)=0, (x_2,y_2)\in S \\ c(x_2,y_2)\neq 0, (x_2,y_2)\notin S \end{cases}, \tag{9}$$

式中：c_1 和 c_2 为常数，表示均匀光斑在 $g(x_2,y_2)$ 范围内的任意位置；振幅 $c(x_2,y_2)$ 是对频域振幅的限制。同理，可得

$$\begin{cases} g(x_2,y_2)\approx E_{\text{uni}}(x_2-c_1,y_2-c_2) \\ \left|g(x_2,y_2)\right|^2\approx\left|E_{\text{uni}}(x_2,y_2)\right|^2 \end{cases}。 \tag{10}$$

通过空域 DOE 相位 $\exp[\mathrm{i}\varphi(x,y)]$ 和频域振幅限制条件 $c(x_2,y_2)$ 共同作用实现光束整形，基础 GS 算法与改进 GS 算法比较示意图如图 4 所示，其中 IFFT 为快速傅里叶逆变换。

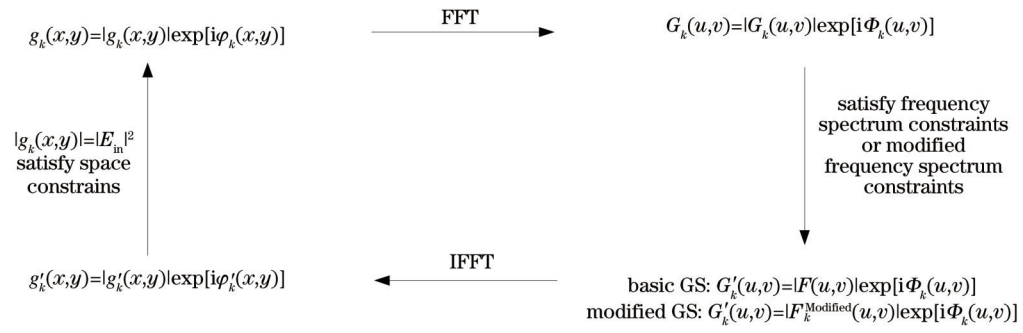

图 4　基础 GS 算法与改进 GS 算法对比图

Fig. 4　Comparison between basic GS algorithm and improved GS algorithm

基于图 4 所示的原理，改进 GS 算法中频域振幅限制[18]为

$$F_k^{\text{Modified}}(u,v)=\begin{cases}2c(u,v)\left|F(u,v)\right|-\left|G_k(u,v)\right|, & (u,v)\in S\\ \left|G_k(u,v)\right|, & (u,v)\notin S\end{cases},\tag{11}$$

式中：$|F(u,v)|$为目标均匀光斑光强；$c(u,v)$的定义为

$$c(u,v)=\frac{\sum\left|G_k(u,v)\right|}{\sum\left|F(u,v)\right|},\ (u,v)\in S。\tag{12}$$

将 2.2 节中基础 GS 算法得到的相位作为初始相位代入改进 GS 算法中，迭代 30 次后结果收敛，光束整形效果如图 5 所示，并计算了均匀度评价参数。仿真结果表明，利用基础 GS 算法结合改进 GS 算法设计的 DOE 得到的均匀光斑光强稳定性和均匀度有很大程度改善，趋于理想均匀程度。矩形均匀光斑长为 28.68 μm，陡度为 89.52°。平顶区域宽度为 17.8 μm（占直径比为 62.06%），U_{ni}=0.0299，E_{RMS}=0.0567，已能满足一般工业加工需求。

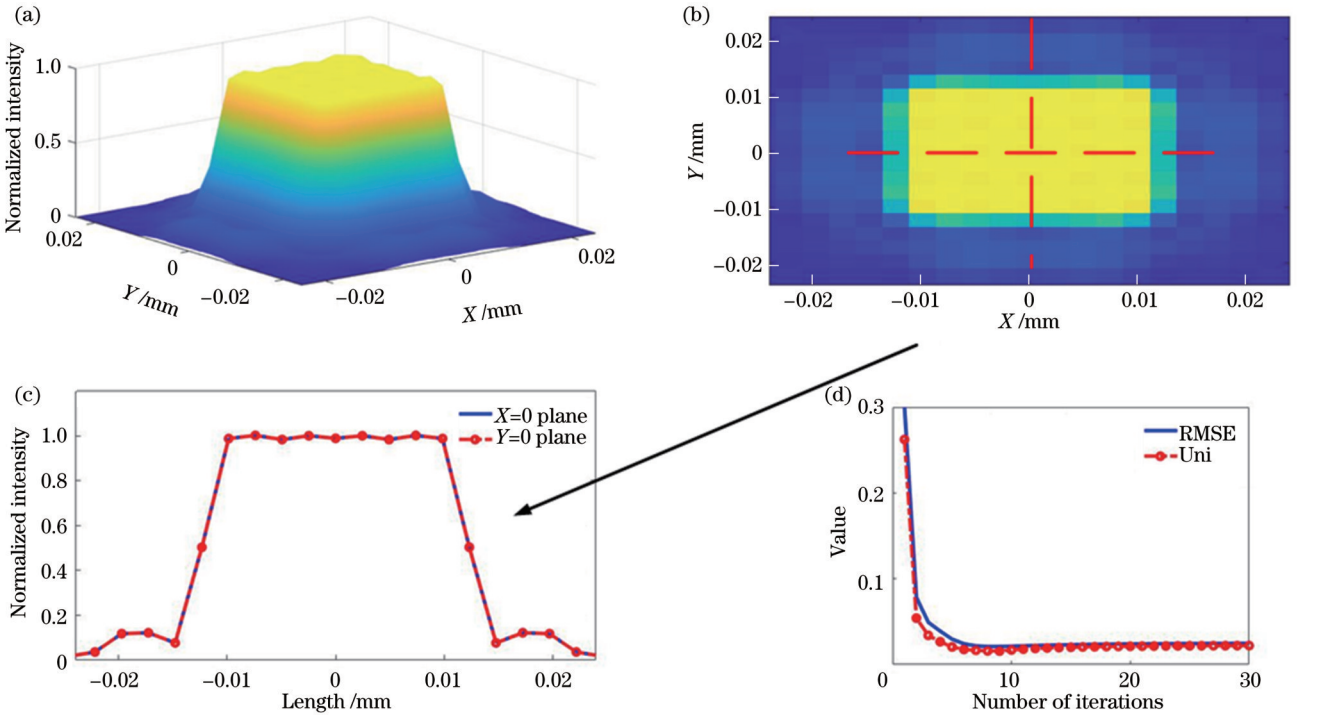

图 5　改进 GS 算法光束整形效果。(a)均匀光斑三维光强分布；(b) XY 平面光强二维分布；(c)坐标轴光强包络曲线；(d) Uni 与 RMSE 随迭代次数收敛的曲线

Fig. 5　Beam shaping effect of modified GS algorithm. (a) Three-dimensional light intensity distribution of uniform spot; (b) two-dimensional distribution of light intensity in XY plane; (c) light intensity envelope curves of coordinate axes; (d) curves of Uni and RMSE converging with number of iterations

在光学系统未引入 DOE 元件之前，该系统的衍射极限（DL）为

$$L_{\text{D}}=M^2\frac{4F_{\text{EL}}\lambda}{2\pi w_0},\tag{13}$$

式中：M^2为光束质量因子；F_{EL}为有效焦距（即为 F）。文中设定 $M^2\approx1$，产生的 DL 为 22.6 μm，故 DOE 只能制备直径大于 22.6 μm 的均匀光斑。然而，本文的目标光斑是边长为 28 μm 的方形均匀光斑，故理论上具备可行性。尺寸越接近 DL，设计难度越大。换言之，目标光斑尺寸与 DL 相差越大，该算法整形效果越好，如该系统制备直径为 50 μm 的均匀光斑，平顶占直径比为 75.68%，U_{ni}=0.0258，E_{RMS}=0.0428，此时整形效果优于制备直径为 28 μm 的均匀光斑。

综上所述，基础 GS 算法结合改进 GS 算法制备均匀光斑相较解析方法而言，存在的优势为：设计目标均匀光斑尺寸、形状更灵活，甚至可以设计无规则形状；均匀光斑的陡度、均匀性和能量利用率有所提升。

3　影响因素分析及实验验证

使用基于所提方法设计的 DOE 时需严格符合设计参数，尤其是 λ、F_{EL}、w_0 三个参数，通常 M^2、λ、F_{EL} 参数确定后不轻易更改，但探测器位置容易出现偏差，故需要仿真分析探测器离焦对整形效果的影响。

3.1　离焦影响

光束整形系统示意图如图 6 所示。激光器出射光束，经过扩束器后光束直径被调整至符合 DOE 设计参数，然后光束经过扫描镜与场镜组合，CCD 相机或者光束质量分析仪放置在场镜后方（距离为 z）。在理想情况下，$z=F$。在离焦情况下，设离焦量为 $\Delta z=z-F$，表示实际距离与场镜理想后焦面位置的差值。

DOE元件表面是高度不同的微浮雕结构，贴合实际加工工艺，仿真中将连续DOE相位进行64台阶灰度量化，其相位灰度图如图7所示。基于上述设定，仿真分析离焦对光束整形效果的影响。

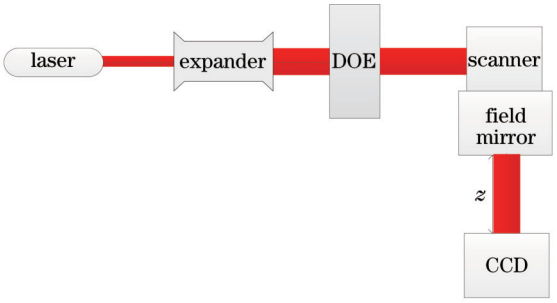

图 6 光束整形系统示意图

Fig. 6 Schematic diagram of beam shaping system

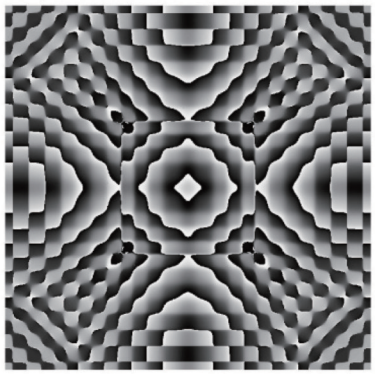

图 7 DOE相位64台阶量化灰度图

Fig. 7 64-step quantized grayscale of DOE phase

基于灰度量化DOE进行离焦误差分析，离焦会导致均匀光斑发生形变，破坏了过渡区和平顶区边界分明的光强分布，故在直径范围内计算评价参数Uni和RMSE，详细数据如表1所示。当$|\Delta z|$达到0.5 mm时，均匀光斑劣化严重以致无法使用，无参考价值，故未记录在表1中。仿真结果如图8所示，左侧为XY二维平面光强分布，右侧为两个坐标轴光强包络曲线。当探测器沿着光束传输方向远离几何焦点($\Delta z>0$)时，均匀光斑光强向中心集中，平顶区域缩小，中心区域能量所占比例越大，光斑尺寸会略微变大。当探测器靠近DOE方向($\Delta z<0$)时，即探测面在几何焦点之前时，能量集中在方形边缘4个角落位置处，平顶区域出现光强较弱的“塌陷”结构。边长为28 μm的方形均匀光斑对离焦误差较为敏感：当$|\Delta z|<20$ μm时，该结构仍能维持平顶光束结构，Uni下降至7.31%左右，RMSE下降至10.62%左右；当离焦量Δz继续增加时，光强均匀度劣化严重，无法满足使用要求。在实际应用中，应尽可能降低探测器误差影响，故在使用DOE之前需要先进行焦面校准工作。

3.2 实验验证

根据图7所示DOE灰度量化后的形貌分布，委托相关合作单位进行加工制作，该单位采用激光灰度直写加工技术制作元件，将实际元件放入光学系统中进行实验验证。选用紫外皮秒脉冲激光器作为光源，选择放大倍数为1～3的变倍扩束镜，以及JENar公司的扫描镜和场镜。观察微米级光斑对相机分辨率要求较高，故采用间接观察法，利用均匀光斑烧蚀样品表面。为了增加样本数据量，间隔相同时间移动样品，在样品表面留下阵列排布的烧蚀“浅坑”，用显微镜观察样品表面烧蚀结果。实验光学系统参数与仿真设定相同，将CCD放置在不同位置来观察离焦情况的实验结果，在显微镜中截取部分光斑，如图9所示。

表 1 离焦对均匀光斑的影响

Table 1 Influence of defocus on uniform spot

Δz /mm	Uni	RMSE
−0.20	0.3933	0.5308
−0.10	0.2294	0.3639
−0.03	0.1285	0.2154
0	0.4999	0.7196
0.03	0.1900	0.3162
0.10	0.3523	0.5518
0.20	0.6451	0.9339

预先对光学系统进行校正，未加入DOE元件之前，根据聚焦光斑尺寸确定几何焦面位置，将DOE元件放入光路中后，校正DOE元件位置和倾斜等空间变量。由实验结果得到：几何焦面($\Delta z=0$)情况中，均匀光斑方形主瓣尺寸为28.59 μm；烧蚀表面较为平整可反推光斑能量密度较均匀，估算均匀性为$U_{ni}\approx10.56\%$和$E_{RMS}\approx12.48\%$；出现旁瓣的原因可能是DOE元件硬边光阑的衍射作用，故最终相位调制作用未能与理想结果一致。调整样品摆放位置，完成离焦实验：当离焦量为$\Delta z<0$时，光强集中在4个顶点位置；当离焦量为$\Delta z>0$时，旁瓣能量增大，继续增大Δz，光斑尺寸增大，主瓣能量更集中。实验验证得到的离焦对光束整形的影响趋势与仿真分析结果基本一致。在后续工作中将继续探究实验与仿真存在差异地方的原因，如当$\Delta z<0$时，4个顶点位置与仿真中不同。除此之外，DOE元件量化、加工制作引入的误差，以及受实验环境扰动、位移平台精度和显微镜像素精度等多种因素影响，都会造成实验与理论值存在差异。

4 结 论

以基础GS算法与改进GS算法相结合的方式设计DOE相位分布，将直径为3 mm的紫外光源高斯光束整形为边长为28 μm的方形均匀光斑，并通过仿真和实验验证了所提方法的有效性和可靠性。在一定误差范围内，实验结果与理论仿真具有一致性。后续将开展提高DOE在工程应用中光束整形效果的研究工作。本研究可为均匀光斑整形DOE的设计方法和

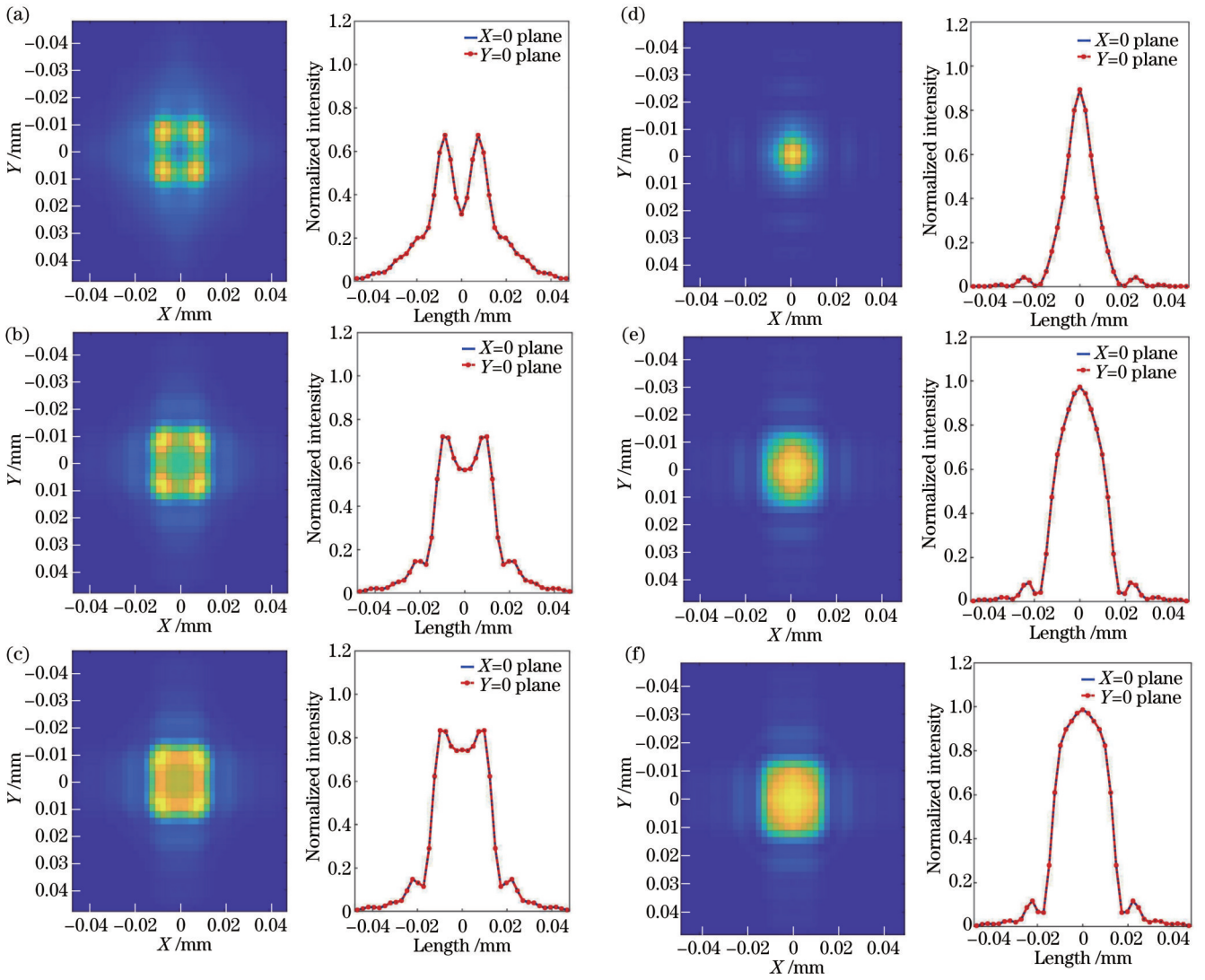

图 8 Δz对光束整形的影响。(a) $\Delta z=-0.5$ mm;(b) $\Delta z=0.5$ mm;(c) $\Delta z=-0.2$ mm;(d) $\Delta z=0.2$ mm;(e) $\Delta z=-0.1$ mm;(f) $\Delta z=0.1$ mm

Fig. 8 Influence of Δz on beam shaping. (a) $\Delta z=-0.5$ mm; (b) $\Delta z=0.5$ mm; (c) $\Delta z=-0.2$ mm; (d) $\Delta z=0.2$ mm; (e) $\Delta z=-0.1$ mm; (f) $\Delta z=0.1$ mm

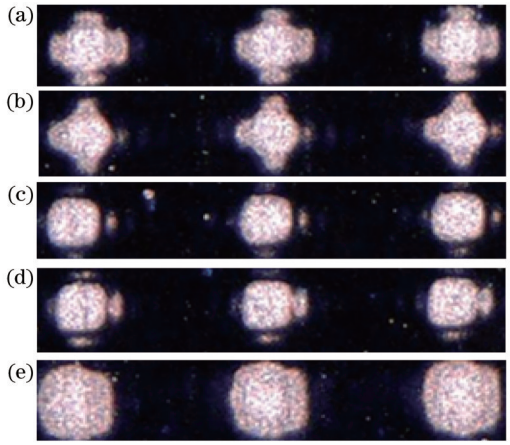

图 9 DOE元件离焦实验结果。(a) $\Delta z=-0.5$ mm;(b) $\Delta z=-0.1$ mm;(c) $\Delta z=0$;(d) $\Delta z=0.1$ mm;(e) $\Delta z=0.5$ mm

Fig. 9 Experiment results of DOE element defocusing. (a) $\Delta z=-0.5$ mm; (b) $\Delta z=-0.1$ mm; (c) $\Delta z=0$; (d) $\Delta z=0.1$ mm; (e) $\Delta z=0.5$ mm

DOE在工程环境中的应用提供数据参考。

参 考 文 献

[1] Geiger M, Popp U, Engel U. Excimer laser micro texturing of cold forging tool surfaces: influence on tool life[J]. CIRP Annals, 2002, 51(1): 231-234.

[2] 孙宁宁, 杨彪, 陈福荣, 等. 激光辅助MicroLED巨量转移技术进展[J]. 中国科学: 技术科学, 2022, 52(4): 513-528.
Sun N N, Yang B, Chen F R, et al. Advances in laser-assisted mass transfer of MicroLED[J]. Scientia Sinica: Technologica, 2022, 52(4): 513-528.

[3] Gauch R, Mikhaylov D, Graf T. Method and device for shaping radiation for laser processing: US20200070280[P]. 2020-03-05.

[4] Voelkel R, Weible K J. Laser beam homogenizing: limitations and constraints[J]. Proceedings of SPIE, 2008, 7102: 71020J.

[5] 彭亚蒙, 苏宙平. 用于发散激光光束整形的自由曲面透镜设计[J]. 光学学报, 2016, 36(5): 0522003.
Peng Y M, Su Z P. Design of freeform surface lens for shaping divergent laser beam[J]. Acta Optica Sinica, 2016, 36(5): 0522003.

[6] 杨向通, 范薇. 利用双折射透镜组实现激光束空间整形[J]. 光学学报, 2006, 26(11): 1698-1704.
Yang X T, Fan W. Spatial laser beam shaping using birefringent lenses[J]. Acta Optica Sinica, 2006, 26(11): 1698-1704.

[7] Laskin A, Laskin V. Imaging techniques with refractive beam shaping optics[J]. Proceedings of SPIE, 2012, 8490: 84900J.

[8] Voelkel R, Herzig H P, Nussbaum P, et al. Microlens array imaging system for photolithography[J]. Optical Engineering, 1996, 35(11): 3323-3330.

[9] 张巍, 梁传样, 李金, 等. 用于激光数字投影显示系统的匀光整形元件设计[J]. 光学学报, 2015, 35(8): 0805001.
Zhang W, Liang C Y, Li J, et al. Design of optical elements for beam shaping and uniform illumination in laser digital projection display system[J]. Acta Optica Sinica, 2015, 35(8): 0805001.

[10] 李昕颖, 钱晓凡, 孟妮妮. 光束整形衍射光学元件的优化算法[J]. 光学学报, 2019, 39(11): 1105003.
Li X Y, Qian X F, Meng N N. Optimization algorithm of diffractive optical elements for beam shaping[J]. Acta Optica Sinica, 2019, 39(11): 1105003.

[11] 林勇, 胡家升, 吴克难. 一种用于光束整形的衍射光学元件设计算法[J]. 光学学报, 2007, 27(9): 1682-1686.
Lin Y, Hu J S, Wu K N. Algorithm for the design of diffractive optical elements for laser beam shaping[J]. Acta Optica Sinica, 2007, 27(9): 1682-1686.

[12] 邬融, 赵东峰, 戴亚平. 并行模拟退火算法优化衍射光学元件设计[J]. 光学学报, 2010, 30(9): 2544-2548.
Wu R, Zhao D F, Dai Y P. Optimize design of diffractive optics elements by parallel simulated annealing[J]. Acta Optica Sinica, 2010, 30(9): 2544-2548.

[13] Laskin A, Laskin V. Method and apparatus for shaping focused laser beams: US09285593B1[P]. 2016-03-15.

[14] Liu J S, Thomson M J, Taghizadeh M R. Automatic symmetrical iterative Fourier-transform algorithm for the design of diffractive optical elements for highly precise laser beam shaping[J]. Journal of Modern Optics, 2006, 53(4): 461-471.

[15] Bryngdahl O. Optical map transformations[J]. Optics Communications, 1974, 10(2): 164-168.

[16] Wyrowski F. Diffractive optical elements: iterative calculation of quantized, blazed phase structures[J]. Journal of the Optical Society of America A, 1990, 7(6): 961-969.

[17] Liu J S, Taghizadeh M R. Iterative algorithm for the design of diffractive phase elements for laser beam shaping[J]. Optics Letters, 2002, 27(16): 1463-1465.

[18] Liu J S, Caley A J, Taghizadeh M R. Symmetrical iterative Fourier-transform algorithm using both phase and amplitude freedoms[J]. Optics Communications, 2006, 267(2): 347-355.

Design of DOE Based on Modified GS Algorithm for Preparation of Micron-Scale Uniform Light Spot in Ultraviolet Band

Zhang Yuying, Zhao Shuai*, Zheng Xin

Ji Hua Laboratory, Foshan 528200, *Guangdong, China*

Abstract

Objective The laser light source is generally Gaussian intensity distribution, and its energy concentration features uneven surface energy density of the sample, material damage, and other problems in the fields of micro-precision machining such as laser drilling, MicroLED repair and transfer, and laser cutting. In this paper, the micron-scale uniform light spot is prepared based on diffractive optical elements (DOEs), and the shape and size of the uniform light spot can be flexibly designed with a high degree of freedom. The difficulty in DOE design for preparing small-sized uniform light spots is to achieve steep and sharp transition areas and characteristic parameters with uniformity of less than 5% in the flat-top area. If the DOE is designed based on the analytical method, the transition area of the uniform light spot changes slowly, and the uniform area effectively used is quite smaller than the diameter. The analytical method is not suitable for preparing small-sized uniform light spots. Therefore, the numerical analysis method is used to design the DOEs. The most effective one is the iterative Fourier algorithm, including the Gerchberg-Saxton (GS) algorithm and its various improved algorithms, which are effective tools in DOE design. Usually, the parameters of the optical system are not easily changed after being determined, but the detector position is prone to deviation. In order to analyze the application of this DOE in the engineering environment, the influence of the defocus on the beam shaping is analyzed through simulation and experiments.

Methods Before the DOE element is introduced into the optical system, the diffraction limit of the system should be calculated, and the DOE can only prepare a uniform light spot larger than the diffraction limit. Based on diffraction limit constraints, an ultraviolet (UV) short wavelength light source is used. This paper combines the basic GS algorithm and the modified GS algorithm. Firstly, the basic GS algorithm is used to calculate the primary phase distribution of DOE. The initial phase will affect the number of iterations and the convergence speed of the GS algorithm. Moreover, it is easy to fall into the local optimal solution. Based on the principle of spatial filtering, the initial phase is calculated, which can reduce the number of iterations. Secondly, this phase is used as the initial phase of the modified GS algorithm. In the frequency spectrum range, the range of the uniform light spot is defined as the signal area S, and the rest of the range is defined as the noise area. The frequency domain amplitudes both in the signal area and the noise area are limited [Eq. (11)]. The beam shaping is realized through the spatial DOE phase and frequency domain amplitude constraints. The schematic diagram of the comparison between the basic GS algorithm and the improved GS algorithm is shown in Fig. 4. According to the beam shaping system (Fig. 6), the analytical method, the basic GS algorithm, and the basic GS algorithm combined with the modified GS algorithm are compared to analyze their effects of beam shaping.

Results and Discussions The size of the uniform light spot prepared based on the analytical method is limited by that of the incident light spot, the parameters of the optical system, etc., and it has strong constraints and can only prepare regular shapes, and simulation results are shown in Fig. 1. Because the size of the uniform spot is close to the diffraction limit, the basic GS algorithm has an unsatisfactory shaping effect and does not change the Gaussian intensity distribution. As a result, it cannot meet the parameter requirements, and the Gaussian beam cannot be shaped into a uniform spot only by the phase of the blazed grating. Therefore, in addition to the phase degree of freedom, the amplitude degree of freedom is added to modify the GS algorithm and improve the beam shaping effect. The basic GS algorithm combined with the modified GS algorithm designs the uniform light spot by DOE, and the light intensity stability and uniformity are greatly improved and tend to become the ideal uniformity (Fig. 5). According to the simulation and experimental results, it is concluded that the defocus leads to the deformation of the uniform spot, which destroys the well-defined light intensity distribution in the transition area and the flat-top area. When the detector is far away from the geometric focus along the beam transmission direction, the spot size becomes slightly larger. The flat-top area shrinks, and the energy in the central area accounts for a large proportion. When the detector is close to the DOE direction, or in other words, the detection surface is in front of the geometric focus, the energy is concentrated in the four corners of the square edge, and the collapsed structure with weak light intensity is in the flat-top area (Fig. 8 and Fig. 9). The square uniform spot with a side length of 28 μm is more sensitive to defocus error. When $|\Delta z|<20$ μm, the flat-top beam structure can still be maintained, uniformity (Uni) drops to about 7.31%, and root-mean-square error (RMSE) drops to about 10.62%. The strength uniformity is seriously deteriorated and cannot meet the requirements of use. In practical applications, the influence of detector errors should be reduced as much as possible, and focal plane calibration should be performed before the DOE is used.

Conclusions In this paper, the DOE phase distribution is designed by combining the basic GS algorithm and the modified GS algorithm, and the Gaussian beam of UV light source with a diameter of 3 mm is shaped into a square uniform spot with a side length of 28 μm. The effectiveness and reliability of the method are verified by simulation and experiments. Within a certain error range, the experimental results are consistent with the theoretical simulations. In the follow-up, research work to improve the beam shaping effect of DOE in engineering applications will be carried out. This paper provides data reference for the design method of uniform spot shaping DOE and the application of DOE in an engineering environment.

Key words laser optics; DOE design; modified GS algorithm; flat-top beam shaping; laser processing